JTTEE5 16:927–932
DOI: 10.1007/s11666-007-9088-6
1059-9630/$19.00 © ASM International

Sliding Wear Properties of HVOF Thermally Sprayed Nylon-11 and Nylon-11/Ceramic Composites on Steel

L. Jackson, M. Ivosevic, R. Knight, and R.A. Cairncross

(Submitted March 9, 2007; in revised form June 21, 2007)

Polymer and polymer/ceramic composite coatings were produced by ball-milling 60 μm Nylon-11 together with nominal 10 vol.% of nano and multiscale ceramic reinforcements and by HVOF spraying these composite feedstocks onto steel substrates to produce semicrystalline micron and nanoscale reinforced polymer matrix composites. Room temperature dry sliding wear performance of pure Nylon-11, Nylon-11 reinforced with 7 nm silica, and multiscale Nylon-11/silica composite coatings incorporating 7-40 nm and 10 μm ceramic particles were characterized using a pin-on-disk tribometer. Coefficient of friction and wear rate were determined as a function of applied load and coating composition. Surface profilometry and scanning electron microscopy were used to characterize and analyze the coatings and wear scars. The pure Nylon-11 coating experienced less wear than the composites due to the occurrence of two additional wear mechanisms: abrasive and fatigue wear.

Keywords HVOF spraying of polymers, Nylon-11, sliding wear, wear resistance

1. Introduction and Background

According to Brostow, wear is the progressive loss or damage of the operating surface of a body occurring as a result of relative motion at the surface (Ref 1). The reduction of surface wear is a common goal in many industries. Frequently repairing or replacing worn parts costs businesses both time and money. Therefore, producing more durable polymeric coatings for applications such as protecting machine parts would significantly broaden the marketability of thermally sprayed polymers.

Wear and surface damage are the outcome of numerous factors, including various wear mechanisms, atmospheric degradation and applied loads. The wear mechanisms mostly associated with sliding contact with polymers are adhesion, abrasion, and fatigue (Ref 2). Adhesive wear results from opposing surface asperities coming into contact under load and undergoing shearing and/or plastic deformation. One asperity may be torn away from its base, generating wear debris if the interfacial bonding is stronger than the cohesive bonding in one material (Fig. 1).

Abrasive wear is the effect of a third body or asperity from one material sliding or rolling in contact with the surface of another forming a groove. The groove is a consequence of material being plowed or pushed to the side and deforming plastically, or the removal of surface material. Fatigue wear causes cracks on and within a coating. Cyclic stresses or cyclic thermal loading and intersecting stress fields slowly deform materials and weaken their surface cohesion. Over time, cracks will open, propagate and material will be pulled out from the surface. This weakening also contributes to adhesive and abrasive wear (Ref 3).

The role of friction in wear couples is defined by the delamination theory of wear as having a significant effect on the wear rate due to surface traction on the plastically deformed asperities and crack propagation rate (Ref 2). Friction can be described in terms of a coefficient of sliding friction, μ, defined as:

$$\mu = \frac{F}{W} \quad \text{(Eq 1)}$$

where F is the tangential force required to maintain tangential relative motion between the two surfaces and W the normal load pressing the surfaces together. However, surface roughness, sliding speed, temperature, relative humidity, the true area of contact, and load intensity also contribute to the coefficient of friction (CoF).

One possible way to improve the sliding wear resistance of polymers is to reinforce the polymeric matrix using a hard

This article is an invited paper selected from presentations at the 2007 International Thermal Spray Conference and has been expanded from the original presentation. It is simultaneously published in *Global Coating Solutions, Proceedings of the 2007 International Thermal Spray Conference*, Beijing, China, May 14-16, 2007, Basil R. Marple, Margaret M. Hyland, Yuk-Chiu Lau, Chang-Jiu Li, Rogerio S. Lima, and Ghislain Montavon, Ed., ASM International, Materials Park, OH, 2007.

L. Jackson, Department of Materials Science and Engineering, North Carolina State University, Raleigh, NC, USA; **M. Ivosevic** and **R. Knight**, Department of Materials Science and Engineering, Drexel University, Philadelphia, PA, USA; and **R.A. Cairncross**, Department of Chemical and Biological Engineering, Drexel University, Philadelphia, PA, USA. Contact e-mail: knightr@coe.drexel.edu.

particulate ceramic phase such as silica or alumina. The addition of nano and micron-sized silica particles has been shown to increase scratch resistance when added to Nylon-11 (Ref 4). HVOF sprayed Nylon-11 with 10 vol.% of 7 nm silica has been previously tested. The study concluded that the composite reinforced coatings exhibited improved sliding wear resistance, however, it was also noted that changes in crystallinity can also influence the wear behavior (Ref 5). G. Srinath reported a 28% decrease in the CoF of Nylon-66 after the addition of 20% glass fibers (Ref 6). The dry sliding wear tests were conducted under similar conditions to those of this research.

The incorporation of multiscale particulate ceramic materials into a polymer matrix may greatly influence the wear behavior of the composite coating. The aim of this research was to compare the sliding wear behavior of pure Nylon-11, Nylon-11 reinforced with 10 vol.% of 7 nm silica alone and Nylon-11 with 10 vol.% of 7 to 40 nm + 10 μm silica, on the basis of CoF, wear scar depth and wear mechanisms.

2. Experimental Approach

2.1 Materials Selection and Coating Production

Industries use Nylon-11, a thermoplastic polyamide, for coatings due to its favorable properties including its semicrystalline structure and good resistance to chemical corrosion (Ref 7). Nylon-11 also has a broad temperature range over which the material can be used. Its melting point is ~183 °C, but Nylon-11 does not degrade until it reaches temperatures between 360 and 550 °C (Ref 8). Nylon-11 (Rilsan Natural D60 ES, Arkema, Inc., King of Prussia, PA), was used as the matrix material for the nano and multiscale composite coatings due to the wide array of industrial applications of Nylon-11 and its inherent properties. The mean Nylon-11 particle diameter was 60 μm with a particle size range of 10 to 180 μm (Ref 4). The size of the Nylon-11 particles used was large relative to that of the ceramic reinforcements. This size differential played a significant role during the feedstock preparation when the smaller ceramic reinforcements were embedded into, or formed a ceramic-rich cladding around, the softer, coarser polymer matrix.

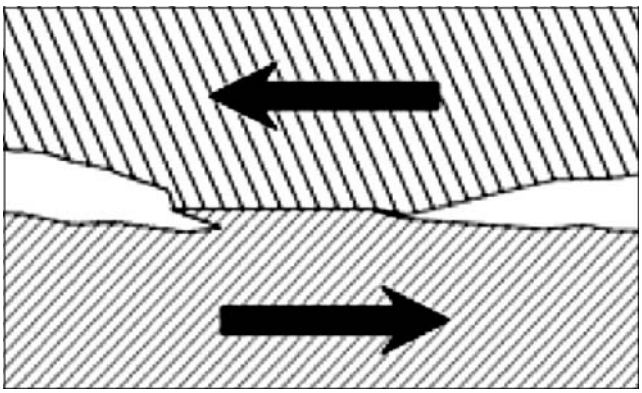

Fig. 1 Schematic of adhesive wear. Both surfaces undergo plastic deformation and during sliding, one asperity may remain adhered to the other surface and be torn from its original surface

Aerosil® fumed silica (Degussa, Piscataway, NJ) was used as the reinforcing material in both the nano and multiscale composite coatings because of its high-specific surface area (~380 m^2/g) and hardness (Ref 9). Results of hardness tests carried out on fumed silica similar to that used in this work indicated hardness values of the order of ~6 GPa (Ref 10). These properties contribute to the sought-after reinforcing characteristics because a high surface area allows for a greater matrix/reinforcement interaction and the increased hardness makes the silica more resistant to permanent deformation. Plastic deformation plays a large role in the wear behavior; therefore, reducing permanent deformation may reduce the wear rate. The silica particles used ranged from 7 to 40 nm and 10 μm in diameter.

Composite feedstock powders were produced by combining Nylon-11 and nano or multiscale silica in a 9:1 ratio by volume. The compositions of the polymer and polymer/ceramic powders used are summarized in Table 1. The nominal 10 vol.% multiscale reinforcement comprised equal proportions of each of the five particle sizes, phyically blended prior to ball milling. Each composition was ball-milled for 48 h using zirconia balls to ensure sufficient embedding/coating of the softer Nylon-11 with the silica. Following milling, the composite powders were screened using a coarse mesh sieve to remove the milling balls, and then vacuum dried for an additional 48 h to remove any moisture that the silica may have absorbed/adsorbed from the surrounding atmosphere.

A Jet Kote II® HVOF combustion spray system (Stellite Coatings, Inc., Goshen, IN) was chosen since this process had been previously used to successfully spray Nylon-11 and Nylon-11/silica composites (Ref 11). At temperatures above 360 to 550 °C, Nylon-11 begins to oxidize and degrade (Ref 8). Owing to the high-melt viscosity of the polymer, the semimolten particles need high kinetic energy in order to deform and flow sufficiently on impact with the substrate. Particle speeds in an HVOF gun are typically in the range of 200 to 1000 m/s, generally higher than those associated with plasma or wire-arc spray (Ref 11). The high velocity of HVOF reduces the length of

Table 1 Composition of polymer-composite feedstock powders

Material system	Polymer matrix (90 vol.%)	Silica reinforcement content (10 vol.%)
Pure Nylon-11	Nylon-11 (D60)	...
7 nm (Nanoscale)	Nylon-11 (D60)	Silica (7 nm)
Multiscale (MS)	Nylon-11 (D60)	Silica (7, 12, 20, 40 nm and 10 μm in equal 2.0 Vol. % amounts)

Table 2 HVOF spray parameters

Parameter	Value
Hydrogen flow rate, m^3/s	4.7×10^{-3}
Oxygen flow rate, m^3/s	3.1×10^{-3}
Carrier gas	Ar
Carrier gas flow rate, m^3/s	4.7×10^{-4}-6.28×10^{-4}
Powder feed rate, g/min	4-1.2
Spray distance, m	0.229
Surface speed, m/s	15-50%
Number of passes	5-9

time the polymer particles are exposed to temperatures above their degradation point and reduces the amount of degradation compared to other spray methods which do not accelerate particles as rapidly.

The pure Nylon-11, nano, and multiscale composite powders were fed into the HVOF system using a Praxair Model 1207 volumetric powder feeder (Praxair Surface Technologies, Inc., Indianapolis, IN). Argon was used as the carrier gas at a flow rate of 4.7×10^{-4} m^3/s. Table 2 summarizes the key HVOF spray parameters used during this work (Ref 4).

4140-Steel wear disks 60 mm in diameter and 3.5 mm thick with a central countersunk hole for attaching them to the wear tester were used as the substrate. The disks were roughened prior to spraying by grit blasting using 1500 μm angular alumina grit from a Trinco 24/BP2 (Fraser, MI) grit blasting system to generate a rough surface for the semimolten particles to mechanically adhere to.

The disk substrates were preheated to 200 °C from the rear surface using an electric resistance heater, which was turned off immediately prior to spraying. Temperature was monitored using a type K Chromel/Alumel thermocouple probe. Preheating ensured that the Nylon-11 particles remained in a semimolten state and allowed the particles to flow together on impact at the substrate forming a continuous coating.

After spraying, the coatings were polished manually on a Struers, Inc. (Westlake, OH) *Abrapol* metallographic polishing machine using 320-grit (36 μm) SiC paper to remove the as-sprayed roughness. Surface roughness can greatly impact the rate at which the topmost surface wears and affect the overall wear behavior. In this case, however, the roughness of the polished surfaces was not measured or quantified further.

Thermal spraying involves many process variables, which affect the structure and properties of the resulting coatings. These characteristics include oxidation due to in-flight and postdeposition heating of the polymer, porosity, and widely varying levels of crystallinity. Each variation and combination can affect the wear behavior of the resulting coating. In order to minimize the influence of the variables introduced during spraying, control samples of each powder composition were produced by melt-pressing. 4140-Steel wear disks were placed in the press and preheated to 150 to 200 °C so that the molten polymer would adhere directly to the disk. The control samples were prepared from the same feedstock powders as used for thermal spraying and were melt-pressed at 150 to 200 °C under nominal pressure for 5 min.

Table 3 Sliding wear test parameters

Normal load, N	Sliding speed, m/s	Wear track radius, mm	RPM	Total revolutions
10	0.47	21	213	10,000
20	0.47	17	263	10,000
30	0.47	25	179	10,000

2.2 Wear Testing of Polymer and Composite Coatings

An AMTI (Watertown, MA) pin-on-disk tribometer, controlled *via* a National Instruments (Austin, TX) LabVIEW™ interface, was used to characterize the sliding wear performance of the thermally sprayed and melt-processed samples. Coated disks were attached to a circular turntable via a central countersunk screw. A 10 mm diameter single crystal sapphire ball was used as the counterbody. Each disk was rotated for 10,000 rotations with the counterbody applying a constant normal load. Coatings were tested using loads of 10, 20, and 30 N. A constant sliding speed of 0.47 m/s was selected and maintained throughout each test. Full wear test parameters are summarized in Table 3. The wear tester calculated and recorded the CoF at a sampling rate of 1 Hz.

2.3 Wear Scar Characterization

Following each wear test, wear track depth was measured using a Hommelwerke (Villingen-Schwenningen, Germany) Dektak-II stylus-tracing profilometer with a stylus tip radius of 0.5 μm. The surface profilometer was calibrated using a glass standard with a known scratch depth of 10 μm.

Scanning electron microscopy was performed on the thermally sprayed coatings using an FEI (FEI Company, Hillsboro, OR) model XL-30 field emission environmental scanning electron microscope. Prior to SEM analysis the Nylon-11 and composite coatings were sputter coated with platinum for 20 s using a Denton (Denton Corp., NJ) Desk-II sputtering system.

3. Results and Discussion

3.1 Coefficient of Friction

Analysis in the results was based upon observed variations between the different coating systems in terms of CoF, wear track depth, and SEM analysis of the wear scars. Results from the pin-on-disk testing exhibited similar trends for each coating when tested using a 10 N load. An initial break-in period was observed in each case, during which the sapphire ball wore through the outermost surface layer, smoothing out any residual surface irregularities, during which the CoF increased steeply. The CoF value of each coating subsequently reached a plateau value in the range 0.25 to 0.40 after ~3,000 rotations. Results at a load of 20 N generally exhibited longer break-in periods and lower CoF values, with the multiscale composite coating exhibiting the highest CoF of ~0.26. At

a load of 30 N, the HVOF sprayed pure Nylon-11 coating had the highest CoF, ~0.38 (Fig. 2). Results of the average CoF for each coating after 3000 rotations are shown in Table 4. In order to verify the repeatability of the sliding wear tests and CoF measurements, three different disks of each thermally sprayed multiscale composite coating were tested at wear track radii of 17, 21, and 25 mm using a 20 N applied load. Statistical analysis of the final 6,000 rotations of each wear test indicated a mean CoF of 0.266 with a standard deviation of 0.017, indicating a high degree of sample-to-sample and test-to-test repeatability.

Data and trends for the CoF were largely inconclusive with regards to wear behavior. While the HVOF sprayed 7 nm composite coating had deeper wear tracks than the HVOF sprayed pure Nylon-11 under 10 and 20 N loads, their CoF values exhibited no significant differences. Under a 30 N force, however, the CoF of the HVOF sprayed pure Nylon-11 coating was almost twice that of the HVOF sprayed 7 nm composite coating. The wear track in the sprayed 7 nm composite coating at 30 N was, however, deeper than that worn in the pure Nylon-11. The CoF between two materials is often assumed to be the same and independent of the value of applied load, however, comparing the values of the CoF of sprayed pure Nylon-11 under the three loads used showed that CoF varied with applied load. Therefore, these results indicated that more factors influenced the CoF than just the normal and tangential loads.

Table 4 Average CoF value after 3000 rotations

	10 N	20 N	30 N
Pure Nylon -11	0.280	0.220	0.386
7 nm Composite	0.273	0.232	0.235
Multiscale Composite	0.381	0.258	0.257

3.2 Wear Scar Depth

Results from the stylus tracing profilometer indicated the depth of each wear track. For the thermally sprayed coatings, the multiscale composite coating had the deepest wear tracks under 10 and 20 N applied loads. The sprayed 7 nm composite coating had the deepest track (~102 μm) at 30 N applied load. A summary of the results for all the thermally sprayed coatings is shown in Fig. 3.

For the melt-pressed coatings, the 7 nm reinforced composite coating had 148 μm deep wear track under a 10 N applied load, and the multiscale reinforced composite coating had a 167 μm deep wear track for a 20 N applied load. The wear tracks on the melt-pressed multiscale composite coating at 30 N load and the 20 and 30 N load wear tracks for the melt-pressed 7 nm reinforced composite coating were greater than 200 μm in depth, outside the range (200 μm max.) of the stylus-tracing profilometer, and could not be measured. Results from the analysis of wear scar depth of the melt-pressed coatings are shown in Fig. 4.

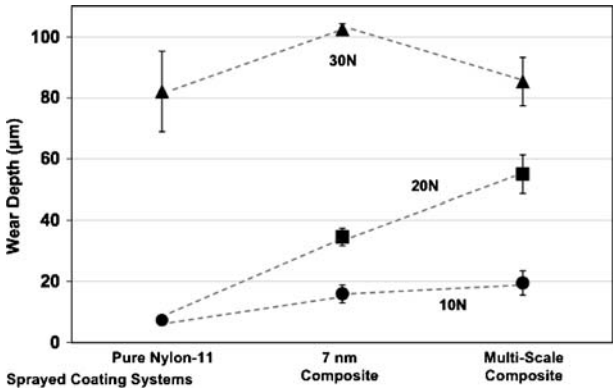

Fig. 3 Comparison of wear track depth for all the thermally sprayed coatings

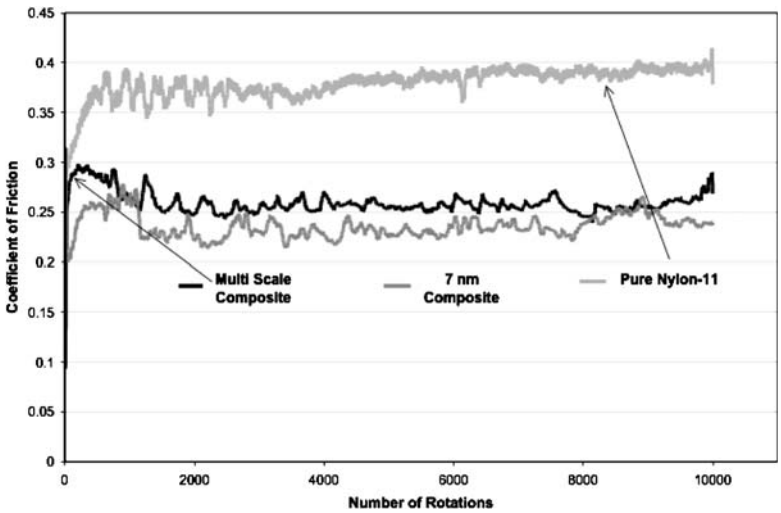

Fig. 2 Coefficient of friction vs. number of rotations for HVOF sprayed coatings under a 30 N applied load. The pure Nylon-11 coating (lightest gray line) had the highest CoF at ~0.38

Wear scar depth is a good indicator of wear rate since it can quantify the volume of material lost due to under sliding wear conditions. Of all the sprayed coatings, the pure Nylon-11 exhibited less wear than the composite coatings. The pressed coatings followed the same trend of decreasing wear resistance for the composite coatings.

3.3 Scanning Electron Microscopy

SEM analysis of the wear scars in the different coating samples revealed evidence of various wear mechanisms. Images of the pure Nylon-11 coatings predominantly showed smearing of material in the wear track. A few pieces of free and unattached wear debris and surface cracks were observed (Fig. 5). Large pieces of loosely adherent rolled and smeared debris were also observed on all three coatings, as shown in Fig. 6. The two sprayed composite coatings showed signs of abrasive and fatigue wear (Fig. 7 and 8, respectively). Further analysis of the coating microstructure by optical microscopy revealed grooves as likely evidence of abrasive wear (Fig. 9). Figure 9 shows a micrograph of a polished cross section of a sprayed coating, with nonuniformly distributed silica reinforcement-rich regions clearly visible in the microstructure, together with polymer-rich regions and some porosity, all of which could have influenced or favored crack propagation.

Examination of the wear scar depth data in the context of the wear mechanisms observed in the SEM images allowed a possible explanation of the decrease in wear resistance observed for the composite coatings to be postulated. Signs of wear due only to adhesion were observed

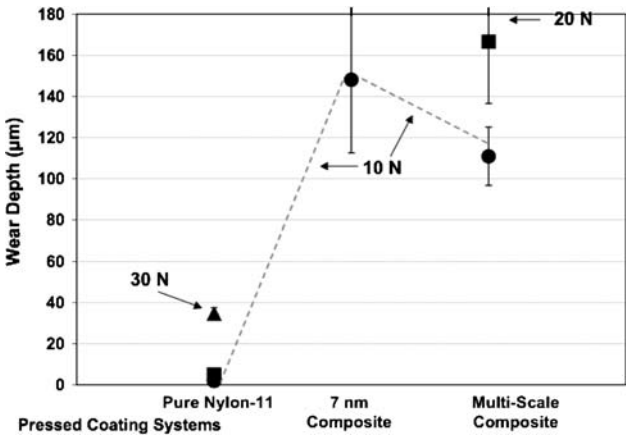

Fig. 4 Comparison of wear scar depth for melt-pressed coatings

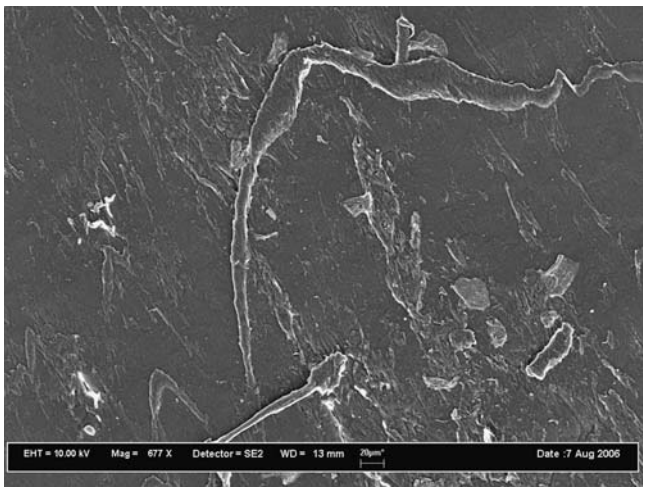

Fig. 5 SEM image of the wear track in an HVOF sprayed pure Nylon-11 tested at 20 N load. Most of the wear debris was adherent to or smeared across the surface such as the large curved debris shown in this image

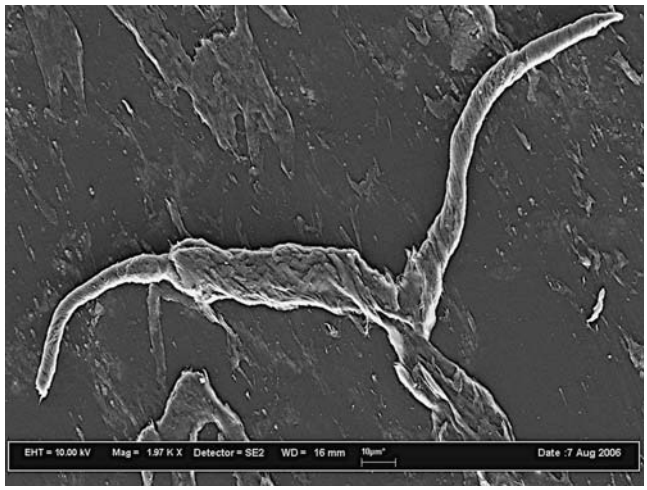

Fig. 6 SEM image of the wear track in an HVOF sprayed 7 nm reinforced composite coating tested at 20 N load. This type of rolled debris was observed in all the coatings and was possibly a result of adhesive wear

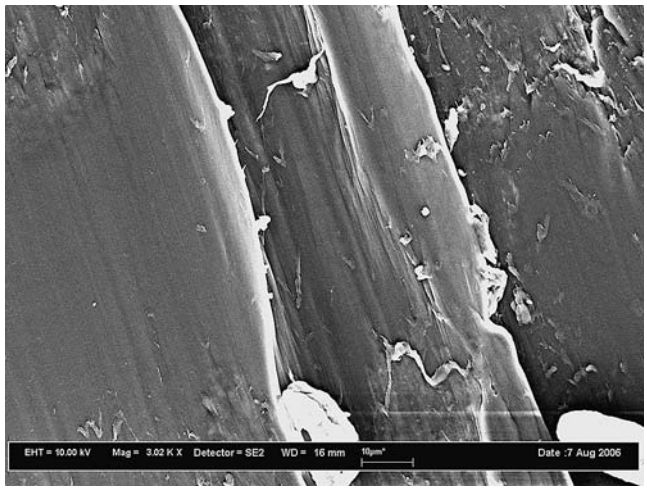

Fig. 7 SEM image of the wear track in an HVOF sprayed 7 nm reinforced composite coating tested at 30 N load. The two grooves running diagonally across the image were the result of abrasive wear. The white regions were pieces of wear debris left in the bottom of the grooves

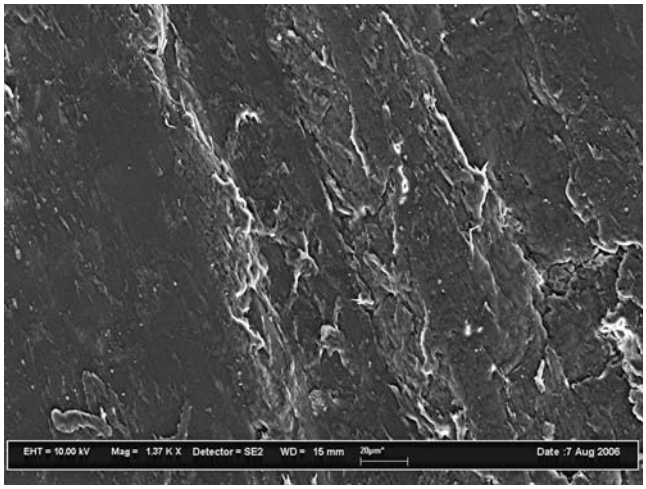

Fig. 8 SEM image of the wear track in an HVOF sprayed multiscale reinforced composite coating tested at 30 N load. A large crack is visible in the lower right corner of the image and smaller cracks throughout, possibly the result of fatigue wear. The cracks are the result of cyclic loading and were only seen in the composite coatings

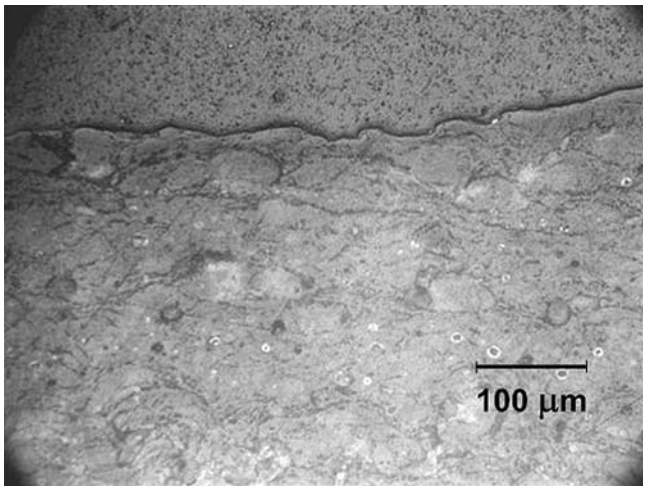

Fig. 9 Optical micrograph of the crosssection of an HVOF sprayed multiscale composite coating taken at a magnification of 200×. Signs of abrasive wear, seen as grooves at the bottom of the wear track are evident in the upper center of the image

in the pure Nylon-11 coatings. In the composite coatings, however, abrasive and fatigue wear also took place (Fig. 7 and 8). The abrasion was likely caused by the particulate silica being pulled out from the polymer matrix and subsequently acting as third bodies. These loose particles could then remove more polymer matrix and silica as they were rolled or pushed across the surface of the coating by the sapphire ball. The pure Nylon-11 coating lacked these hard particles and therefore, had nothing comparable to effectively cut into or plow through the polymer coating. The pure Nylon-11 was primarily smeared under the sapphire counterbody and little material was actually removed from the surface.

4. Summary and Conclusions

These results contradicted previous indications that Nylon-11 coatings reinforced with 7 nm silica exhibited greater sliding wear resistance than pure Nylon-11. The same study, however, revealed that the crystallinity of the polymer matrix played a significant role in the wear behavior (Ref 5), and it is believed that this may have contributed to the behavior observed in this case. Further evaluations are required in order to determine how the level of crystallinity influences the wear behavior regardless of the loading and size scale of the particulate reinforcements.

Acknowledgments

The authors would like to thank the National Science Foundation for providing support for this research under collaborative grant number DMI 0209319 and grant number NSF EEC 0353922. The views expressed in this paper do not necessarily reflect those of NSF. The authors also greatly appreciate the assistance and help of Mr. Dustin Doss and Mr. Steve Niezgoda during the HVOF spraying of the coatings, Mr. Aaron Sakulich during the microscopy and microstructural analysis and Mr. Mark Shiber for machining.

References

1. W. Brostow, G. Darmarla, J. Howe, and D. Pietkiewicz, Determination of Wear of Surfaces by Scratch Testing, *E-Polymers*, 2004, **3**, p 8
2. D.A. Rigney, Fundamentals of Friction and Wear of Materials. ASM International®, Materials Park, OH, USA, 1981
3. N.K. Myshkin, Tribology of Polymers: Adhesion, Friction, Wear and Mass-Transfer, *Trib. Int.*, 2005, **38**(11), p 910-922
4. V. Gupta, Thermal Spraying of Polymer-Ceramic Composite Coatings with Multiple Size Scales of Reinforcement, M. S. Thesis, Drexel University, Philadelphia, PA 2006
5. E. Petrovicova, Structure and Properties of Polymer Nanocomposite Coatings Applied by the HVOF Process, Ph.D. dissertation, Drexel University, Philadelphia, PA 1999
6. G. Srinath, Effect of Short Fiber Reinforcement on the Friction and Wear Behavior of Nylon-66, *Appl. Compos. Mater.*, 2005, **12**(6), p 369
7. H. Chen, H. Zhao, J. Qu, and H. Shao, Erosion-Corrosion of Thermal-Sprayed Nylon Coatings, *Wear*, 1999, **233-235**, p 431-435
8. M.I. Kohan, Nylon Plastics Handbook. Hanser Gardner Publications, New York, USA, 1995
9. Degussa Corporation, Aerosil and Silanes, 2 Turner Place, Piscataway, NJ 08855
10. L.M. Yang, Y.J. Wang, Y.W. Sun, G.S. Luo, and Y.Y. Dai, Synthesis of Micrometer-Sized Hard Silica Spheres with Uniform Mesopore Size and Textural Pores, *J. Colloid Interface Sci.*, 2006, **299**(2), p 823-830
11. E. Petrovicova and L.S. Schadler, Thermal Spraying of Polymers, *Int. Mater. Rev.*, 2002, **47**(4), p 169-190